FAULT ANALYSIS OF VENUS RIDGE BELTS NEAR APHRODITE TERRA. J. A. Balcerski[1], P. K. Byrne[2], [1]Ohio Aerospace Institute, Cleveland, OH. (jefferybalcerski@oai.org), [2]Planetary Research Group, Department of Marine, Earth, and Atmospheric Sciences, North Carolina State University, Raleigh, NC.

Introduction: Ridge belts on Venus tend to be narrow, heavily lineated, positive-relief features generally tens of kilometers wide, up to thousands of kilometers in length, and having vertical expressions of hundreds of meters [e.g. 1–3]. These belts often border and delineate expansive lower-lying and relatively featureless plains and frequently occur in association with tesserae and other areas of relatively high surface deformation. Some have been identifiedas "dorsae". The relative timing of formation of ridge belts does not appear to be confined to a specific chronologic period, nor is there a clear universal relationship between belt formation, local radar-bright lineaments, surrounding terranes, and other regional structures [2]. Mechanisms of formation are difficult to determine from the Magellan Global Topographic Data Record (GTDR) data, but the recent availability of stereo-derived topography (stereotopo) for ~20% of the planet at an optimal resolution of 1–2 km/px [4] provides an opportunity to differentiate between symmetric and asymmetric ridges (thus informing interpretation of volcanic constructive/spreading centers versus collisional/compressive mechanisms), and to develop a better understanding of the relationship between radar-bright lineations, the topographic ridge expression, and surrounding topography.

Location: Since the region around Aphrodite Terra is well-represented in the stereotopo data set we searched for linear, topographic ridges across which detailed profiles could be acquired, as shown in Figure 1. We selected those features that were at least identifiable in the Magellan GTDR product and well-resolved in the Herrick et al. [4] model, as well as the 75 m Magellan FMAP mosaics. This feature set includes both identified dorsae and unnamed but morphologically similar ridges. In all cases, the profiled features bear characteristics similar to the "broad arch" categorization of Frank and Head [2], with an average width around 50 km and length of about 1500 km.

Process: We constructed several topographic profiles oriented as close to perpendicular to the belt strike as the stereotopo data permitted. These data have spatial resolutions that are highly variable, so we selected profiles from those locations with the highest resolution (in this case, ~1.5 km/px). The resulting profiles were compared with those over the same sections taken with GTDR data (~ 5 km/px). With the increased resolution provided by the stereotopo data, we were able to compare locations of the radar-bright parallel/subparallel lineations within the belt structure with the topographic expression of the belt. These profiles were then inspected for any apparent (a)symmetries; where possible, ridge slopes were also measured.

Topographic analysis*:* Although data from the GTDR are insufficient to distinguish between symmetric and asymmetric character of the ridge, the stereo data clearly show that the ridges are composed of asymmetric flanks with multiple peaks and valleys (Figure 2). In general, ridges are also characterized by the presence of narrow (< 10 km) valleys on one or both sides of the ridge, with much more broad depressions at a distance of 100–200 km from the ridge center. In all cases, the ridge represents a notable positive topographic deflection in otherwise flat or subdued terrain. Given the strikingly similarity to lunar and Martian wrinkle ridges [2, 5–8], we use a similar numeric elastic continuum model as previous studies [e.g., 9] to place estimates on the subsurface geometry of the underlying fault(s).

Results: The features profiled here are remarkably similar, in morphology and aspect ratios of (cross-strike) width-to-maximum height, to those of earlier studies [10,11]. The isolated nature of the ridges and the presence of intraridge peaks and valleys are remarkably similar to terrestrial mountain ranges and implies a similar mechanism of construction (e.g., orogeny). Crustal shortening along a décollement is likely implicated as a major process given the canonically inferred low water content of Venusian crustal materials [e.g., 12], and as the planet's surface is equivalent to a low metamorphic grade environment, it is unlikely that this detachment surface exists because of volatile pore pressure or poorly consolidated strata. We presume that this surface more likely represents Venus' relatively shallow brittle–ductile transition [e.g., 13], at least in the lowlands where these ridge belts are predominantly situated. The results of our use of the COULOMB software toolkit to numerically model plausible fault geometry largely support this interpretation: our best-fit models suggest that these ridges are fault-related folds atop an extended horizontal thrust fault at around 9 km below the surface, which terminates about 3 km below the ridge (Figure 3). In contrast to earlier models (of ridges with narrower cross-strike width), these models here imply fault stuctures at greater depth with greater horizontal displacement along the nearly-horizontal fault. Given our previous work, we infer that although the constructional

mechanisms are similar, there is a direct relationship between the overall width of ridge belts and the depth of faulting needed to generate them. This implies that large listric thrust faults sole (i.e., bottom out) at varying depths of confinement across Venus. This inference, in turn, implies either a compositionally hetereogeneous crustal material and/or an internal heat flux that varies with either time or location.

References: [1] Barsukov, V. L. et al. (1986). *JGR, 91, D378-398.* [2] Frank, S. L. and Head, J. W. III. (1990). *Earth, Moon, and Planets, 50/51,* 421-470. [3] McGill, G. E. and Campbell, B. A. (2006). *JGR, 111, E12006.* [4] Herrick, R. R. et al. (2012). *EOS, 93, No. 12,* 125-126. [5] Watters, T. R. (1988) *JGR Solid Earth, v93, B9,* 10236-10254. [6] Golombek, M. P. et al. (1991). *LPSC XXI.* 679-693. [7] Watters, T. R. and Robinson, M. S. (1997). *JGR, v102, E5,* 10889-10903. [8] Golombek, M. P. et al. (2001). *JGR, v106,* 23811-23821. [9] Watters, T. R. (2004). *Icarus, v171,* 284-294. [10] Balcerski, J. A. et al. (2018). *LPSC XLIX,* #2735. [11] Balcerski, J. A. et al. (2018). *VEXAG XVI.* #8012. [12] Barsukov, V. L. et al. (1980). *LPSC XI,* 765-773. [13] Mikhail, S. and Heap, M. J. (2017). *Phys. Of Earth and Planetary Int., v268,* 18-34.

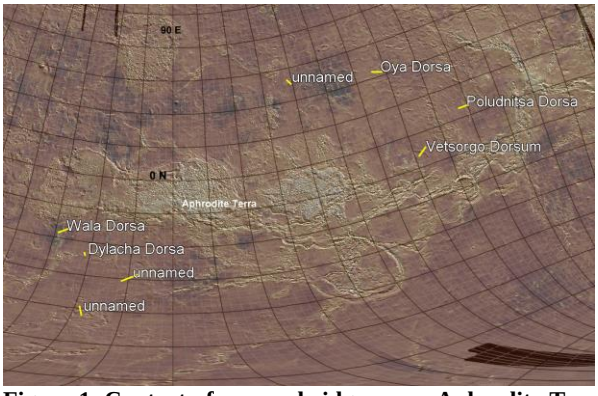

Figure 1. Context of mapped ridges near Aphrodite Terra, Venus.

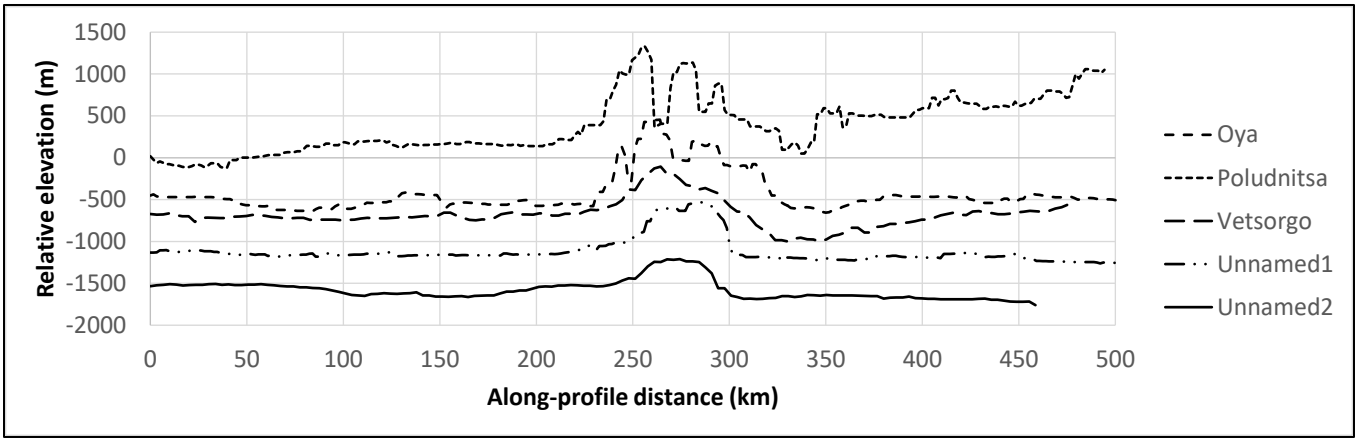

Figure 2. Profiles of mapped ridges. Vertical exaggeration = 70x.

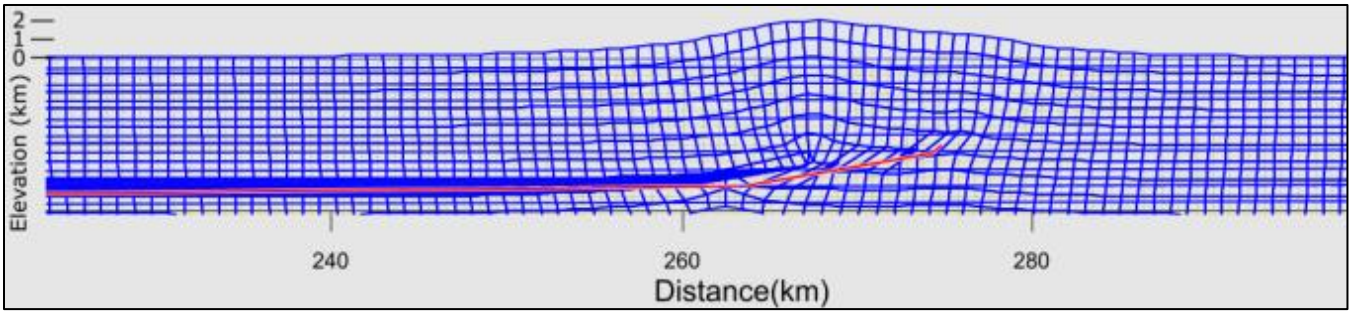

Figure 3. Profile of modeled fault. Vertical exaggeration = 10x.